Cyclic Behavior of Electroslag Welded Joints in Beam-to-Built-Up Box Column Steel Moment Connections

Gulen Ozkula[1]; Rupa Garai[2]; Peter Lee[3]; and Chia-Ming Uang, M.ASCE[4]

Abstract: Steel special moment frames (SMFs) with built-up box columns are often used in taller buildings when two orthogonal axes of participating moment frames intersect. Interior diaphragm (or continuity) plates are usually required to strengthen the column at the beam flanges. A common US practice is to use the electroslag weld (ESW) process to provide complete-joint-penetration (CJP) groove welds connecting the plates to the blindside of the box column after it has been welded closed. Available research in Asia has shown that ESW joints used in this application are vulnerable to brittle fracture. Limited research and guidelines are available in US seismic design codes. The design standard for prequalified connections is primarily developed for SMF connections with wide-flange columns in strong-axis bending. To address the use of large box columns in SMFs with reduced beam section (RBS) connections, a test program with three full-scale specimens was conducted; the depth of the column section also exceeded the prequalification limit. Test results showed that the quality of ESW and SMF joint detailing was crucial for the integrity of the connections. Modifications to ESW detailing and welding process included the use of beveled containment plates intended to delay crack development that might initiate from a notch-like condition inside the flange of the box column. SMF detailing recommendations include an enlarged weld access hole geometry and steel backing treatment of the beam top flange.
DOI: 10.1061/(ASCE)ST.1943-541X.0002409.

Author keywords: Special moment frame; Reduced beam section; Steel moment connection; Box column; Diaphragm plate; Electroslag welding.

Introduction

After witnessing the widespread damage to steel moment frame buildings during the 1994 Northridge earthquake in California, FEMA initiated a comprehensive study of steel special moment frames (SMFs) through the SAC Joint Venture (FEMA 2000a). The Joint Venture focused on wide-flange beams connected to wide-flange columns using fully restrained connections; investigation of built-up box columns was not considered. The use of moment frames constructed with built-up box columns using the electroslag weld (ESW) process was widespread in the United States from the late 1960s through the late 1980s (Chambers et al. 2014). No known failures of connections using a box column were reported following the 1994 Northridge event.

Built-up box cross sections are efficient in controlling seismically induced lateral drifts in two directions when columns of orthogonal moment frames intersect. However, their different shape results in a different path for force transfer between the beam and column. When using a wide-flange column, the high in-plane stiffness of the column web creates stress concentration at the midwidth of the beam flange. When using a box column, stress concentrations occur at both tips of the beam flange because the side walls (i.e., webs) are located on either side of the beam flange (Chen et al. 2004). Because the face wall (i.e., flange) of the built-up box column is pulled in the out-of-plane direction by the beam flange tensile force, continuity (or diaphragm) plates are usually required inside the box column. It is common practice to weld diaphragm plates to the interior side of the built-up box column walls using complete-joint-penetration (CJP) groove welds on three sides of the column. The weld on the remaining (closing) side is made by using the ESW process. Because the inside of the column is not accessible after welding, any steel backing of the ESW joint will remain. Unlike a moment connection with a wide-flange column, in which continuity plates and their welds are accessible and can be easily inspected, the diaphragm plates and their welds in a box column cannot be accessed or visually inspected. As an alternative to the fabrication method mentioned previously, the face plate can be made discontinuous by extending two diaphragm plates to the face of the column. Because this detail requires a total of four CJP welds on the face plate, it is not as cost-effective as the ESW method, and therefore is not commonly used.

Electroslag Welding

ESW processes and techniques have been used since the 1960s in the United States and internationally (Chambers et al. 2014). In the United States, the use of conventional ESW procedures and specifications using consumable oscillating guide tubes are typically qualified by testing as per AWS D1.1 (AWS 2011). US research in the 1990s led to the development of improved ESW methods known as ESW narrow-gap (ESW-NG) components and

[1]Assistant Professor, Dept. of Civil Engineering, Tekirdağ Namik Kemal Univ., Tekirdağ, Turkey. Email: gozkula@nku.edu.tr

[2]Associate Director, Skidmore, Owings and Merrill LLP, San Francisco, CA 94111. Email: rupa.garai@som.com

[3]Associate Director, Skidmore, Owings and Merrill LLP, San Francisco, CA 94111. Email: peter.lee@som.com

[4]Professor, Dept. of Structural Engineering, Univ. of California San Diego, La Jolla, CA 92130 (corresponding author). ORCID: https://orcid.org/0000-0002-8467-9748. Email: cmu@ucsd.edu

Note. This manuscript was submitted on February 6, 2018; approved on March 7, 2019; published online on September 19, 2019. Discussion period open until February 19, 2020; separate discussions must be submitted for individual papers. This paper is part of the ***Journal of Structural Engineering***, © ASCE, ISSN 0733-9445.

procedures qualified by the AASHTO/AWS D1.5M/D1.5 (AWS 2008). The new ESW–NG method allows for narrowing the weld cavity, which results in a reduction of heat input. This results in an increase of deposition, a decreased heat-affected zone (HAZ), and increased notch toughness of ESW welds, while eliminating the need for oscillating guides. Typical US weld cavity or root dimensions for conventional ESW is 31.8–38.1 mm (1.25–1.5 in.) and for ESW-NG it is 19.1–22.2 mm (0.75–0.875 in.). The fabricated test specimens presented in this paper utilized the ESW-NG process in conformance with AWS D1.1 and D1.5 requirements and met the demand critical weld requirements of AWS D1.8 (AWS 2009) and AISC 341 (AISC 2010b).

The ESW process commonly used in Japan and Taiwan is based on a simplified electroslag welding (SESNET) process with a nonconsumable automatically elevating tip, and a nonconsumable nozzle is used to guide the electrode. The SESNET process is highly efficient and saves labor costs. Although the various applications of ESW methods are similar in general technique, they can vary significantly in the amount of heat input, types of consumable or nonconsumable materials and electrode filler metals, weld root width, wire feed speed, and other welding parameters.

Built-Up Box Column Moment Connection Research

Research on steel moment connections with built-up box columns is very limited in the United States. However, according to the review of a large database of box column connections that were primarily tested in Japan and Taiwan, it was concluded that box column connections are expected to provide good seismic performance (FEMA 2000b). This review did not mention the vulnerability of ESW joints for diaphragm plate welding.

Prior to the 1994 Northridge earthquake, Anderson and Linderman (1991) investigated the cyclic behavior of 10 beam-column subassemblages with 279-mm (11-in.) square built-up box columns connected to W16 × 26 or W16 × 40 wide-flange beams. ESW was used when the box columns were stiffened with internal diaphragm plates. Six unstiffened specimens did not use diaphragm plates, two specimens incorporated either exterior stiffeners or beam flange cover plates, and two specimens used interior diaphragm plates with welding simulating the US practice at the time. Because the pre-Northridge style bolted web with welded flange moment connections were used, the dominating failure mode was brittle fracture initiated from the steel backing or the beam web weld access hole. Fracture of the beam flange welds started from the flange tips, where the stress concentration was high. One specimen (Specimen 7), which represented the current design practice, had diaphragm plates that matched the thickness of the beam flange. It was reported that during testing, loud pops were heard but no cracking was evident. It was hypothesized that the pops were due to the formation of cracks in the internal welds between the column wall and the continuity plates. When the thickness of the internal diaphragm plates was reduced by half, another specimen (Specimen 9) experienced local buckling of the diaphragm plates.

Tsai et al. (1992) tested 10 steel box column moment connections with conventional reinforcing details. The built-up box columns ranged from 550 × 550 mm to 900 × 900 mm in size. Premature fracture of the internal diaphragm ESW occurred in two specimens. Chen et al. (2004) tested six moment connections with built-up box columns. Except for one reference specimen, the remaining five specimens had internal diaphragm plates. For each diaphragm plate, an ESW process with nonconsumable elevating tip welding process was used to make a pair of CJP welds. To protect the beam flange CJP welds, vertical rib plates were welded to the beam flanges and column flange plate in the connection region for the latter specimens. Cyclic testing showed that using the lengthened vertical ribs was effective in preventing brittle fracture at the beam-to-column CJP welds. However, one specimen failed prematurely at the ESW joint, indicating that welding diaphragm plates inside the box column was crucial for the integrity of the connection.

Kim et al. (2008) tested two pre-Northridge connections with wide-flange beams and built-up box columns featuring typical details of US construction. The internal diaphragm plates were CJP-welded to the column plates, but no detail of these welds was provided. The thickness of the diaphragm plate [25 mm (1 in.)] was thicker than the flange thickness [19 mm (0.74 in.)] of one beam (W33 × 118), but thinner than the flange thickness [40 mm (1.57 in.)] of the other beam (W36 × 232). Because both specimens experienced brittle fracture in the beam flange CJP welds at a very low story drift angle (less than 0.008 rad), the performance of ESW joints could not be evaluated.

Steel moment-resisting space frames with cold-form hollow structural section (HSS) columns are common in Japan. HSS columns are limited to thicknesses less than 40 mm and dimensions less than 1,000 mm. Due to the size limitations of available HSS sections, it is common to use built-up box columns with internal diaphragms for taller buildings (Nakashima et al. 2000). Song et al. (2011) investigated the fracture behavior of ESW joints in the beam-to-built-up box column connections by monotonic testing and numerical simulation. Charpy V-notch (CVN) tests showed that the notch toughness was the lowest along the ESW fusion line. Biaxial pull-plate tests of the column plate–ESW joint–diaphragm plate assemblies showed two types of fracture. Fracture initiated from the notch-like condition between the column plate and steel backing (or containment plates). Fracture then propagated either along the fusion line within the column plate thickness or into the ESW joint; the former fracture type failed in the elastic range and had little ductility capacity.

Chen and Liang (2011) investigated experimentally and numerically the effect of ESW on the material properties of box column plates. The results showed that the column and diaphragm plate thicknesses were the major factors affecting the cyclic capacity of the connection. To evaluate the effect of a much higher heat input produced by the ESW process, the material properties of the column plate before and after ESW were evaluated by macroetching observation, microstructural observation, and CVN impact tests. Numerical simulation also was conducted, and it was found that the impact of the ESW heat cycle was more significant for thin column plates than for thick ones.

Tsai et al. (2015) reported a statistical evaluation of 22 large-size moment connections with built-up box columns that were tested in Taiwan. Except for five specimens that used cover plates to reinforce the beams, the remaining specimens incorporated RBS in the beams. Diaphragm plates were used in the box column for all specimens. Of these one-sided moment connections, six specimens (four RBS connections and two cover-plated connections) had beams connected to the ESW side of the column. One of these RBS connections and both cover-plated connections failed. The remaining 16 specimens had beams connected to the side where the diaphragm plates were connected to the column plates with the gas metal arc welding (GMAW) process. Of all 22 specimens, 50% of the specimens did not achieve the 0.04-rad story drift angle requirement for SMF applications; the failure rate was higher for RBS connections.

Similar research on the effect of ESW of internal diaphragms on the cyclic response of moment connections with built-up box columns is limited in the United States. AISC (2010a, b) and

AWS (2009, 2011) do not provide any guidelines on the design, fabrication, and welding of diaphragm plates in SMF connections. For bridge applications, AASHTO/AWS D1.5M/D1.5 provides requirements for ESW-NG qualification including notch toughness CVN requirements.

Objective

Three full-scale beam-column subassemblies with RBS moment connection were tested at the University of California San Diego. The objective was to evaluate the cyclic performance of steel moment connections; built-up box columns with ESW also exceeded the prequalified sizes of AISC 358 (AISC 2011) for SMF connections.

Test Program

Test Setup and Test Specimens

The overall geometry of the test setup is shown in Fig. 1. Assuming that the inflection occurred at the midheight of the columns and the midspan of the beam, the test setup simulated a story height of 4,877 mm (16 ft) and a bay width of 9,144 mm (30 ft). Each test subassembly consisted of a W36 × 302 beam and a 610-mm-wide (24 in.) and 914-mm-deep (36 in.) built-up box column fabricated with 51-mm-thick (2 in.) plates. The beam framed into the narrower side of the column. The beam-column assembly represented a portion of a real 24-story building in California. According to AISC 358, the beam size nominally met the prequalification limits, but the depth of the column [914 mm (36 in.)] exceeded the prequalification limit of 610 mm (24 in.). When no more than three moment frame beams framed into a box column, it was possible to position the ESW side to avoid beam moment; this was not the case for some two-way moment connections in the aforementioned building that required four beams to frame into the column from all four sides. To test the most critical condition, for each test specimen the beam framed into the column on the side where ESW existed.

The dimensions of the built-up column and beam sections are provided in Fig. 2 and Table 1. The RBS dimensions are listed in Table 2. The reduction of the total flange width was 31% of the beam flange width for the first two specimens, less than the maximum reduction of 50% permitted by AISC 358. No axial load was applied to the column. The moment ratio for strong column–weak beam check was 4.2. After testing these two nominally identical specimens, the connection for Specimen 3 was modified to increase the flange reduction to 49% such that the force demand to the weld joints was reduced.

As required by AISC 358, the built-up column plates were connected with CJP groove welds in a zone extending 305 mm (12 in.) above and below the beam top and bottom flanges (Fig. 2). Partial-joint-penetration groove welds were used for the remaining length of the welds. The thickness of the internal diaphragm plates was 44 mm (1¾ in.) to match the beam flange thickness [43 mm (1.68 in.)] as required by AISC 341. These plates were CJP-welded to three sides of the column in a commercial fabricator's shop using standard flux-cored arc welding (FCAW) process, whereas the CJP weld on the fourth side was made with an electroslag narrow-gap weld process. The ESW-NG weld was in conformance with specifications AWS D1.1 and AWS D1.5, and met the CVN requirements of a demand-critical weld per AWS D1.8 and AISC 341. The ESW-NG root dimension used was 22 mm (7/8 in.). The weld detail is shown in Fig. 3(a). The ESW was perpendicular to the direction of rolling of the diaphragm plates.

Simulated field welding of the beam-to-column moment connections was performed in the test laboratory by a certified welder with the FCAW process using an E70T-6 (Lincoln NR-305) electrode for flat-position welding and E71T-8 (Lincoln NR-232) electrode for beam web and overhead-position welding. Steel backing was removed only from the beam bottom flange for the first two

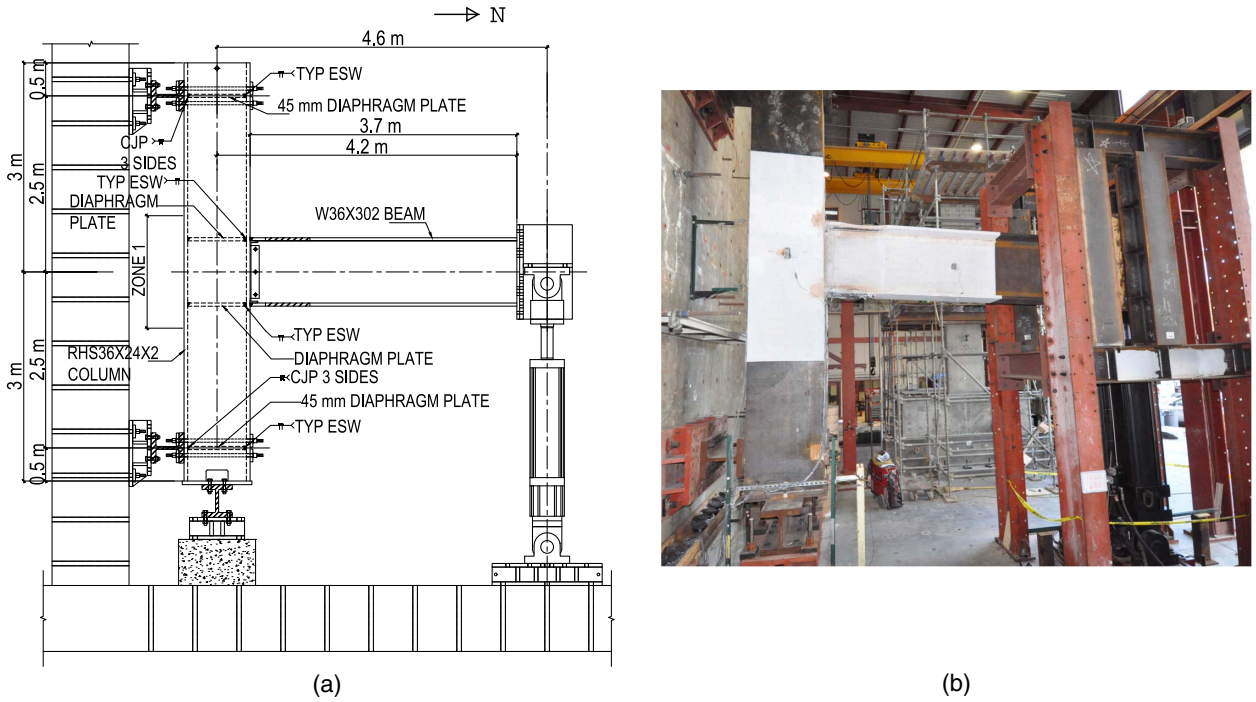

Fig. 1. Test setup: (a) elevation; and (b) specimen prior to testing.

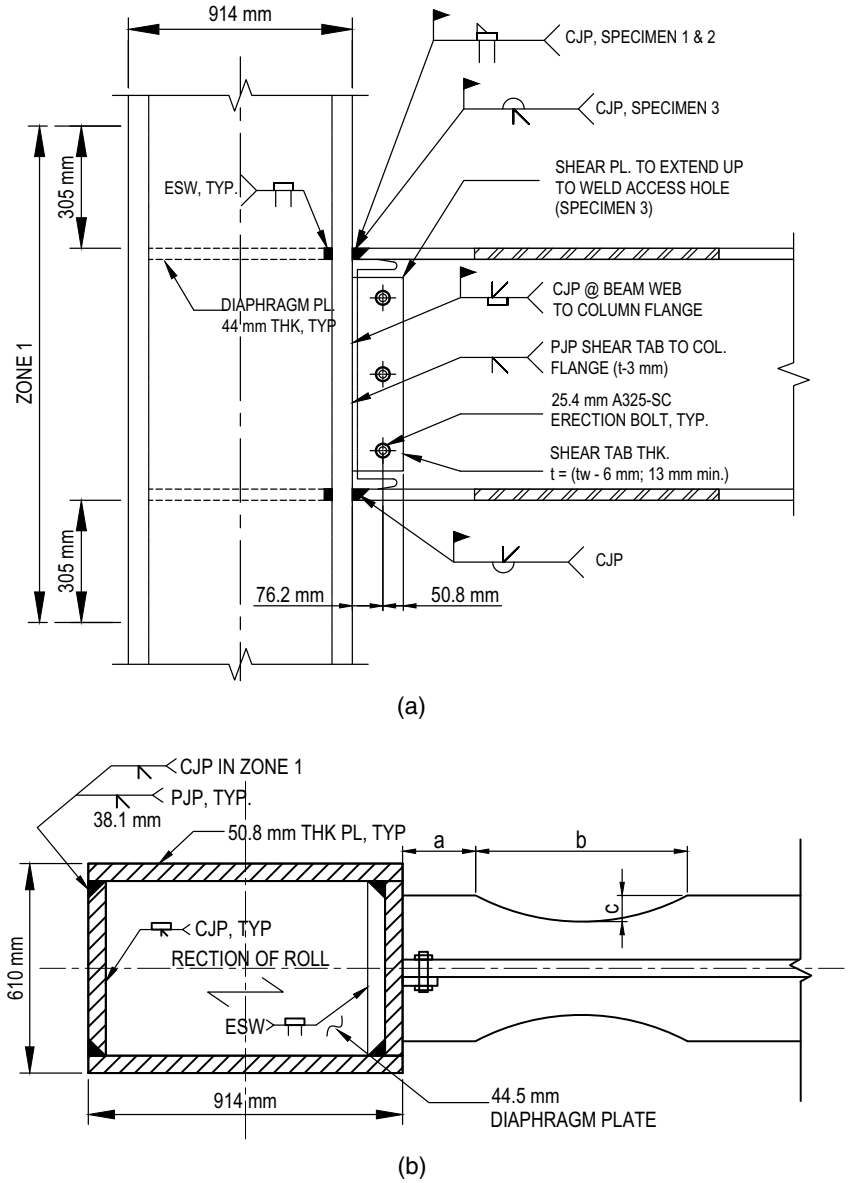

Fig. 2. Box column connection detail: (a) elevation; and (b) plan view.

Table 1. Member sizes

Section	d [mm (in.)]	t_w [mm (in.)]	h/t_w	b_f [mm (in.)]	t_f [mm (in.)]	$b_f/2t_f$
Column (RHS 36 × 24 × 2)	914 (36)	51 (2)	406 (16)	610 (24)	51 (2)	152 (6)
Beam (W36 × 302)	947 (37.3)	24 (0.95)	861 (33.9)	424 (16.7)	43 (1.68)	126 (4.96)

Table 2. RBS dimensions

Specimen No.	a [mm (in.)]	b [mm (in.)]	c [mm (in.)]
1, 2	213 (8–3/8)	616 (24–1/4)	67 (2–5/8)
3	213 (–3/8)	762 (30)	105 (4–1/8)

specimens, as required by AISC 358. Based on the observed crack initiation that originated at the beam top flange backing bar near the flange tips, it was decided to remove steel backing from the top beam flange for Specimen 3. A reinforcing fillet weld was also added after the root pass was backgouged and cleaned. Therefore, Specimen 3 had identical backing bar treatments at both top and bottom flanges.

The weld access hole profile specified as Alternate 1 in Fig. C-J1.2 of AISC 360 (AISC 2010c) or ASW D1.1 was used for the first two specimens. Based on the observed performance of the first two specimens, it was decided to adopt the weld access hole profile specified in Fig. 6.2 of AWS D1.8 for the third specimen; this profile was not required by AISC 358. Based on research of welded unreinforced flange-welded web (WUF-W) connections, this enlarged beam weld access hole geometry permitted improved

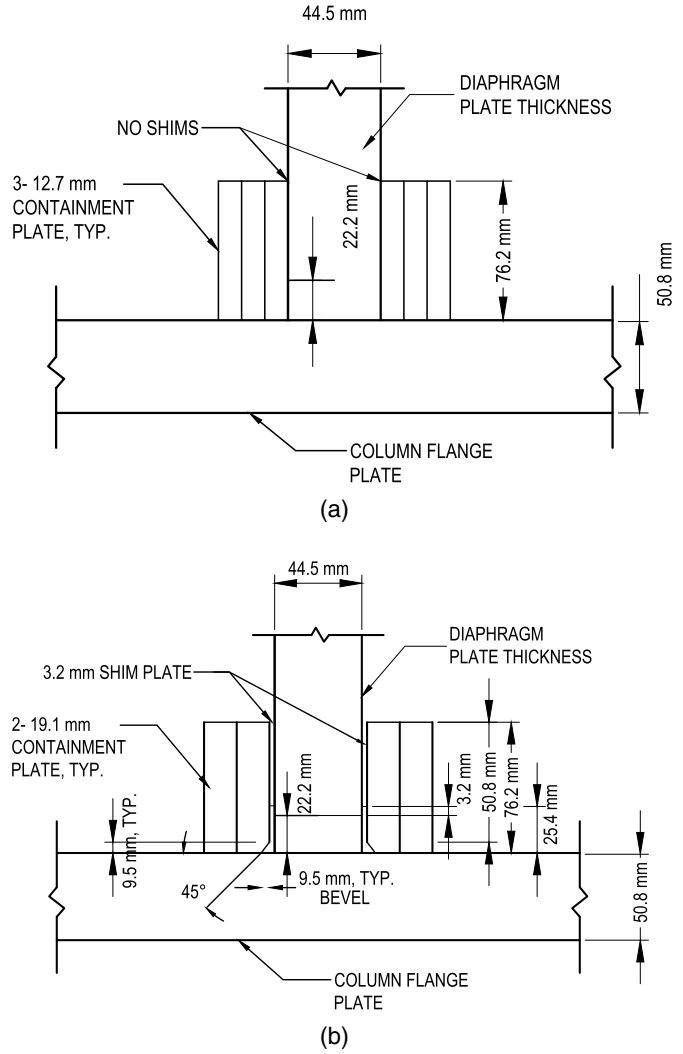

Fig. 3. ESW joint detail: (a) Specimens 1 and 2; and (b) Specimen 3.

performance with more uniform distribution of strains across the column face (Ricles et al. 2002a, b). Lee et al. (2016) showed that this also was true when box columns were used.

Material Properties

ASTM A992 steel with a minimum specified yield stress, F_y, of 345 MPa (50 ksi) was specified for the beam, and A572 Gr. 50 steel [$F_y = 345$ MPa (50 ksi)] was specified for the column plates and diaphragm plates. Table 3 lists the mechanical properties of the steel determined from tensile coupon tests. According to Section A3.3 (Heavy Section) of AISC 341, a minimum Charpy V-notch toughness of 27 J (20 ft-lb) at 21°C (70°F) was required for the W36 × 302 and 50.8-mm-thick (2 in.) plates used in the test specimens; certified mill certificates showed that this requirement was met.

Specimens 1 and 2 Electroslag Welding

For box column fabrication, ESW of the diaphragm plate to the inside column plate at both top and bottom beam flanges was completed using the ESW-NG process and specifications. Prior to welding, the weld procedure specification (WPS) was based on a full-size mock-up of the box column-to-diaphragm plate connection and was qualified by testing in conformance with AWS D1.5 and AWS D1.1. Supporting procedure qualification record (PQR) tests were developed based on a Tee configuration of a diaphragm plate-to-column plate ESW connection.

The ESW-NG process was based on AWS A5.25 specification and EWTG classification filler metal [2.4 mm (3/32 in.) diameter] electrode (Arcmatic VMC 105) and consumable guide tube [31.8 mm (1¼ in.) Arcmatic VS#0233 CS] in the vertical position. Other weld procedure parameters included electrical characteristics of 540–640 A and 38 V, a wire feed speed of 224–279 cm/min (88–110 in./min), and a vertical rate of rise of 2.0 cm/min (0.80 in./min).

Loading Protocol and Acceptance Criteria

Displacement imposed to the beam end corresponded to the cyclic loading sequence specified in Section K2.4b of AISC 341. According to Section E3.6c of AISC 341, beam-to-column connections used in SMFs should satisfy the following requirements: (1) the connection should be capable of sustaining a story drift angle of at least 0.04 rad for one cycle; (2) the required flexural strength of the connection, determined at the column face, should be equal to at least 80% of the nominal plastic moment of the connected beam at a story drift angle of 0.04 rad; and (3) two successful test specimens are required for qualification acceptance.

Test Results of Specimens 1 and 2

The global responses of the first two nominally identical specimens are shown in Figs. 4(a and b); the moment at the column face was normalized by M_{pn}, which is the nominal plastic moment of the beam computed based on a nominal yield stress of 345 MPa (50 ksi). Energy dissipation through inelastic action was mainly from yielding of the beams; panel zones remained elastic and the maximum shear strain reached was about 0.4 times the shear

Table 3. Mechanical properties of steel

Member	Specimen No.	ASTM steel grade	Yield stress [MPa (ksi)]	Tensile strength [MPa (ksi)]	Elongation[a] (%)
Beam flange	1, 2, 3	A992	399 (57.8)	507 (73.6)	33.8
Column plate	1, 2	A572 Gr. 50	393 (57.0)	590 (85.6)	31.5
	3[b]	A572 Gr. 50	431 (62.5)	607 (88.0)	28.5
	3[c]	A572 Gr. 50	414 (60.0)	607 (88.0)	30.5
Diaphragm plate	1, 2	A572 Gr. 50	353 (51.2)	512 (74.3)	33.8
	3	A572 Gr. 50	455 (66.0)	624 (90.5)	30.5

[a]Elongations are based on 203-mm (8-in.) gauge length.
[b]Used at back face and west face of column.
[c]Used at front face and east face of column.

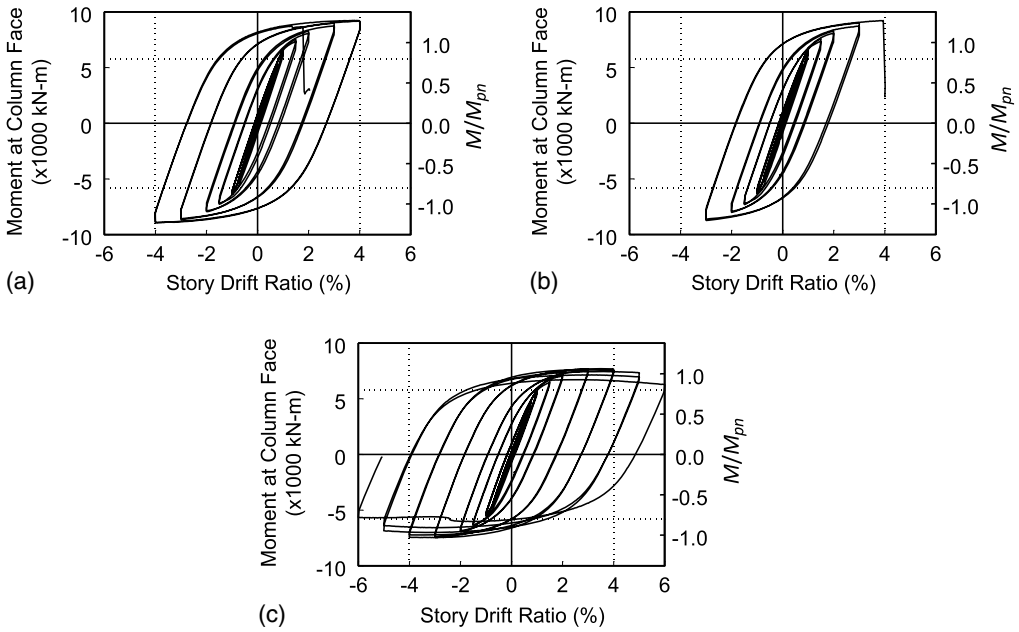

Fig. 4. Global responses: (a) Specimen 1; (b) Specimen 2; and (c) Specimen 3.

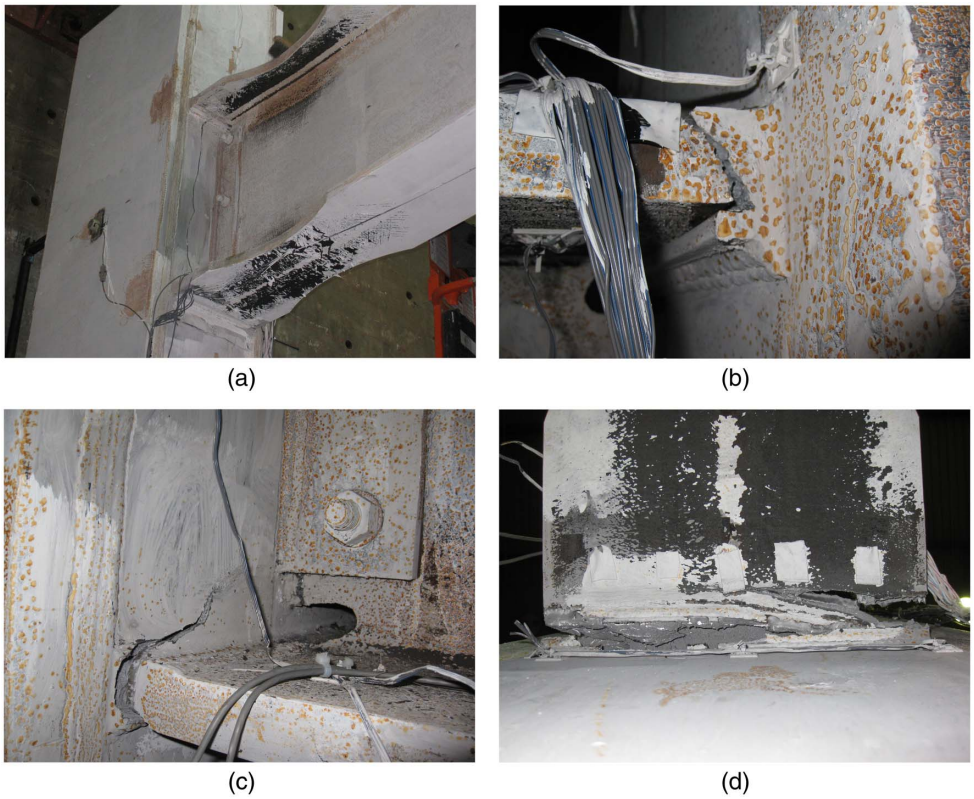

Fig. 5. Specimen 1: (a) yielding pattern; (b) fracture at beam top flange level; and (c and d) complete fracture at beam bottom flange level.

yield strain. Specimen 1 successfully completed two cycles at a story drift angle of 0.04 rad and met the AISC 341 acceptance criteria [Fig. 5(a)]. At a drift level of −0.04 rad (second cycle), a crack at the edge of the beam top flange CJP weld was observed [Fig. 5(b)]. This crack emanated from the backing bar and propagated in the flange thickness direction. This crack initiated at previous drift levels of approximately 0.015–0.02 rad story drift angle. During the first positive excursion to 0.05 rad story drift angle, a brittle fracture occurred at the beam bottom flange level at +0.014 rad drift angle [Figs. 5(c and d)]. This column divot-like brittle failure mode is not typical of an RBS connection behavior (Engelhardt et al. 1998; Yu and Uang 2001). Furthermore, this specimen also did not exhibit typical strength degradation from beam buckling.

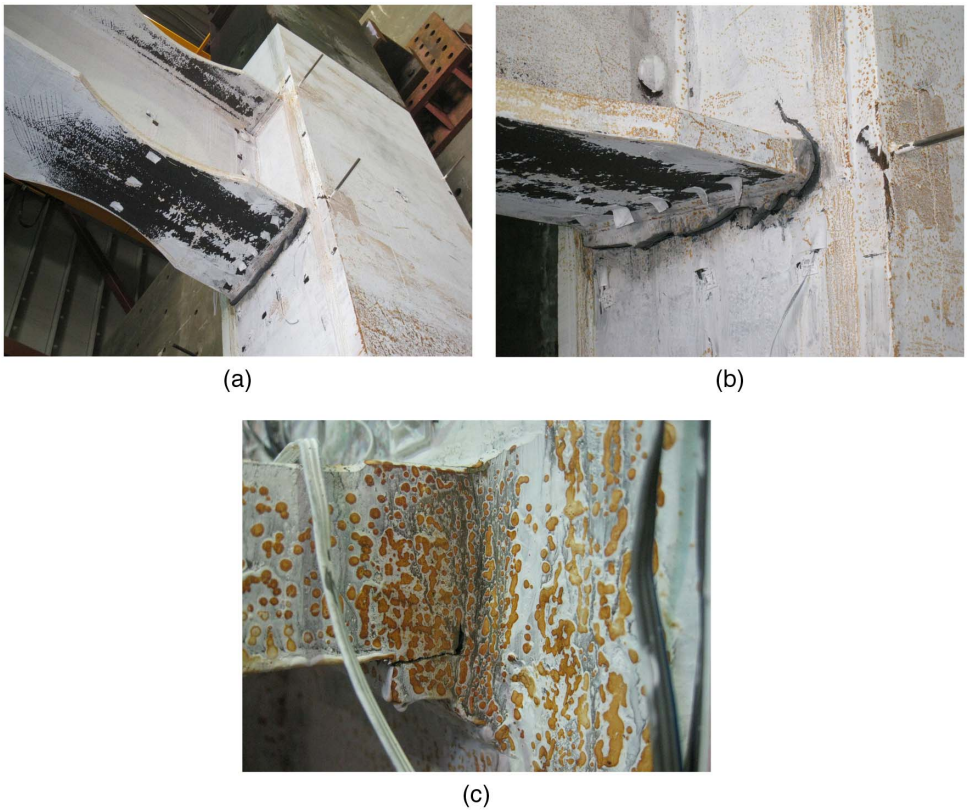

Fig. 6. Specimen 2: (a and b) fracture at beam bottom flange level at +3.9% drift; and (c) fracture at beam top flange level at −3% drift (second cycle).

Specimen 2 similarly experienced a column divot-like fracture at the beam bottom flange level at 0.039 rad drift during the first positive excursion of 0.04 rad drift [Figs. 6(a and b)]. Similar to Specimen 1, a crack initiated at the edge of the top flange from the root of the CJP weld during the 0.02 rad drift cycles. Fig. 6(c) shows the crack at 0.03 rad drift angle.

Analysis of Specimen 1 and 2 ESW Joints

The diaphragm plates and ESW joints at beam flange levels were extracted from Specimens 1 and 2 (Fig. 7). In addition, the diaphragm plate installed near the top end of the column where the column was connected to the reaction wall was detailed and fabricated identically to the moment connection diaphragm plates. Because the column horizontal reaction force exerted to the diaphragm plate at this location was much smaller than that by beam flange forces at the beam-to-column connection region, no damage was expected at this location. These extracted as-built weld joints from Specimen 1 offered an opportunity to examine the diaphragm welds separately from the beam-to-column connection region [Fig. 7(a)]. The diaphragm plate was welded to the column by the FCAW process on three sides, and the last side (closing) side was welded by the ESW-NG process. One slice from the ESW joint was removed for further examination. For comparison purposes, a slice from a FCAW weld joint also was removed. This sampling of Specimen 1 allowed for baseline comparisons with samples taken from the moment connection region of Specimen 2 (Ozkula and Uang 2014).

Specimen 1

Figs. 8 and 9 show the macroetched surface as well as the Rockwell B scale hardness (HRB) profiles across the weld, heat-affected zone, and column flange plate of both the FCAW and ESW weld joints extracted from the top end of the column. The HRB, which is related to the tensile strength, of the ESW joint was similar to that of the FCAW joint (approximately 90) and the hardness of either weld was not significantly higher than that of the base metal. This indicates that the weld metal and its HAZ were not the cause of premature failure of the weld. Fig. 10 shows the microstructures in different parts of the ESW joint. The microstructures were very similar to those found in the FCAW joint.

Specimen 2

Fig. 11 shows the macroetched surfaces of the ESW joints at the top flange level. Although brittle fracture like that at the bottom flange was not observed at the top flange level during test, Fig. 11(c) illustrates the distinct and sharp notches created during shop welding. The notch condition was created at the nonwelded juncture of the ESW containment plates and column flange plate. Furthermore, the ESW joint shifted downward with respect to the diaphragm plate during fabrication, creating a fully fused asymmetric weld. A similar condition was reported by Tsai et al. (2015).

Macroetched surfaces of the welded joint at three locations at the beam bottom flange level are shown in Fig. 12. The cracks initiated from the notches and propagated into the column flange plate. This same brittle fracture mode also occurred at the bottom flange level of Specimen 1.

Connection Modifications for Specimen 3

After analyzing the results of Specimens 1 and 2, the following modifications were made to improve the connection performance.

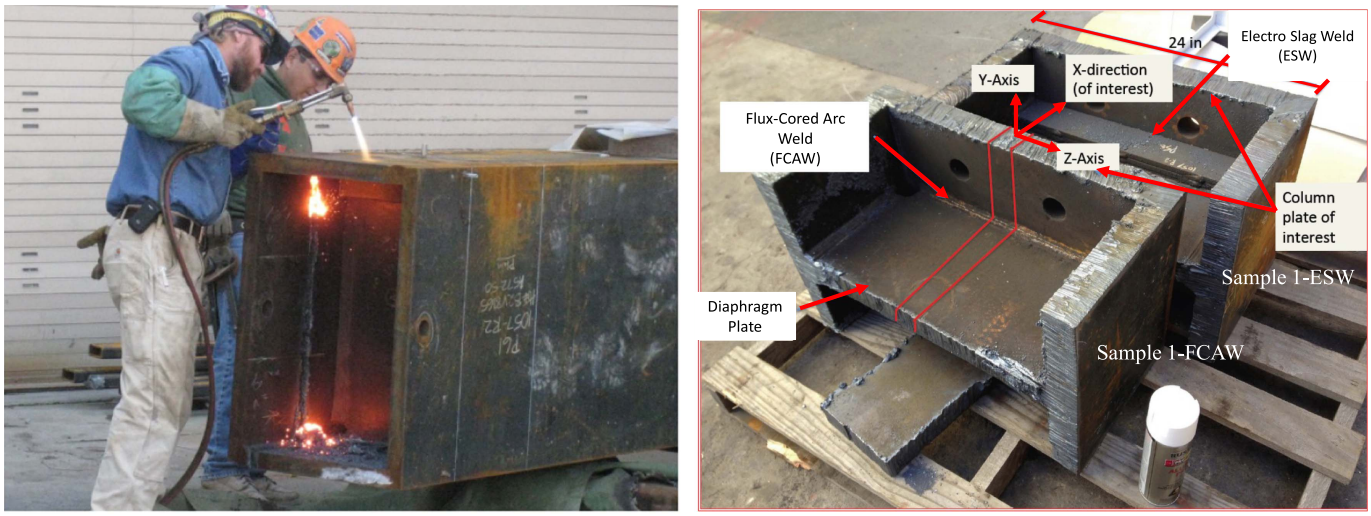

(a)

(b)

Fig. 7. Extraction of diaphragm plate weld samples: (a) Specimen 1; and (b) Specimen 2.

ESW Joint

Weld Detail

The ESW joint details for both Specimens 1 and 2 and the modifications made to Specimen 3 are illustrated in Fig. 3. The weld root gap dimension was 22.2 mm (7/8 in.) for all three specimens. The welded joint consisted of a 50.8-mm (2-in.) column flange thickness and 44.5-mm-thick (1¾-in.) diaphragm plate. For Specimens 1 and 2, the backing on each side of the weld root gap was made up of three 12.7 × 76.2-mm (1/2 × 3-in.) containment plates. To mitigate the notch effect in electroslag welding research in Taiwan, Lin (personal communication, 2013) proposed a beveled profile with a 2:1 slope with dimensions of 20 × 10 mm (0.79 × 0.39 in.) for the innermost containment plates. The weld electrode manufacturer, Arcmatic, recommended two 19.1 × 76.2-mm (3/4 × 3-in.) containment plates on each side of the ESW, with a 9.5 × 9.5-mm (3/8 × 3/8-in.) bevel on the innermost containment plate. Additionally, a 3.2-mm (1/8-in.) shim plate was placed between the inner containment plate and the diaphragm plate, which acted as a spacer plate to both widen the weld cavity and to act as a chill bar. The chill bar allowed the weld to shrink without inducing additional stress and ensured no fusion of the containment plates with the diaphragm plate. Fig. 3(b) shows the revised detail that was incorporated in Specimen 3. The revised details were intended to mitigate cracking from the notch effect. This modified configuration resulted in a smoother transition of the ESW bulb. In addition, the wider ESW bulb provided some redundancy to offset fabrication tolerances between the beam flange and diaphragm plate alignment.

Weld Process

The weld procedure specification for Specimen 3 was re-qualified with supporting procedure qualification record testing in conformance with both AWS D1.1 and AWS D1.5. Other than the modifications made to the ESW containment plates described previously, all parameters of the ESW-NG process remained the same as for Specimens 1 and 2 weld procedure specification, except for the following additional modifications. For Specimen 3, the ESW-NG process again used the same filler metal and consumable guide tube. However, three other weld procedure parameters were modified to improve the quality of the weldment. These included (1) reducing the electrical voltage input from 38 to 35 V, (2) reducing the vertical rate of rise from 0.80 to 0.60 in./min, and

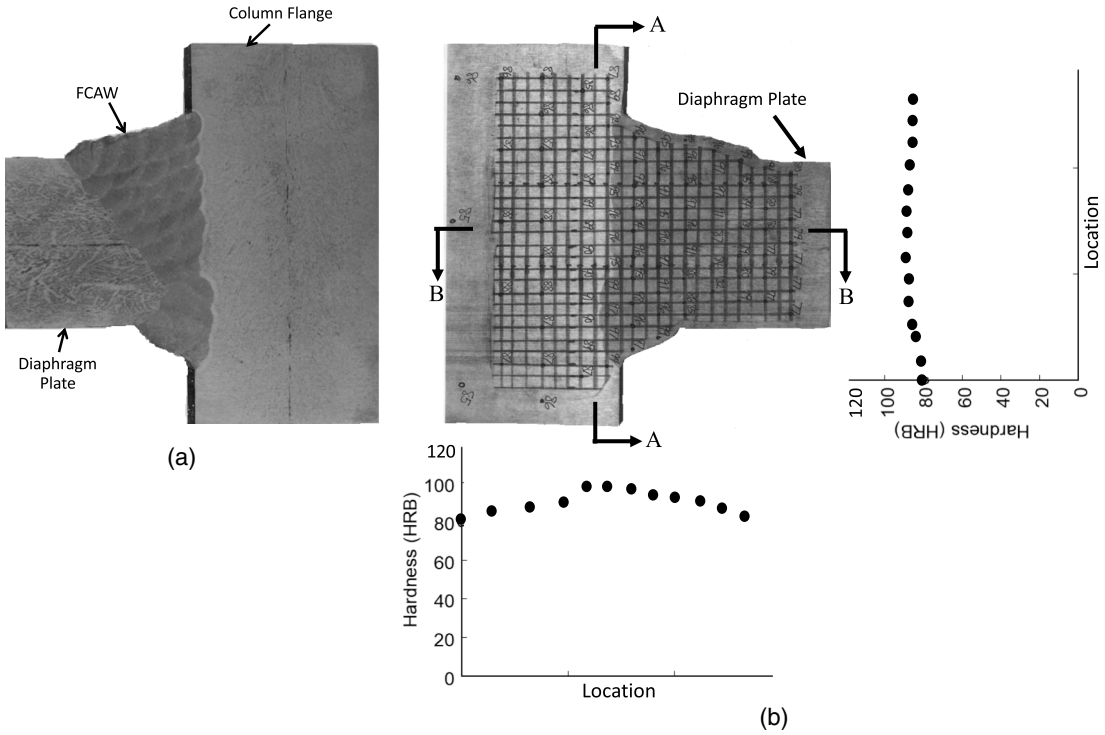

Fig. 8. Specimen 1 FCAW joint: (a) macroetched surface; and (b) Rockwell B scale hardness.

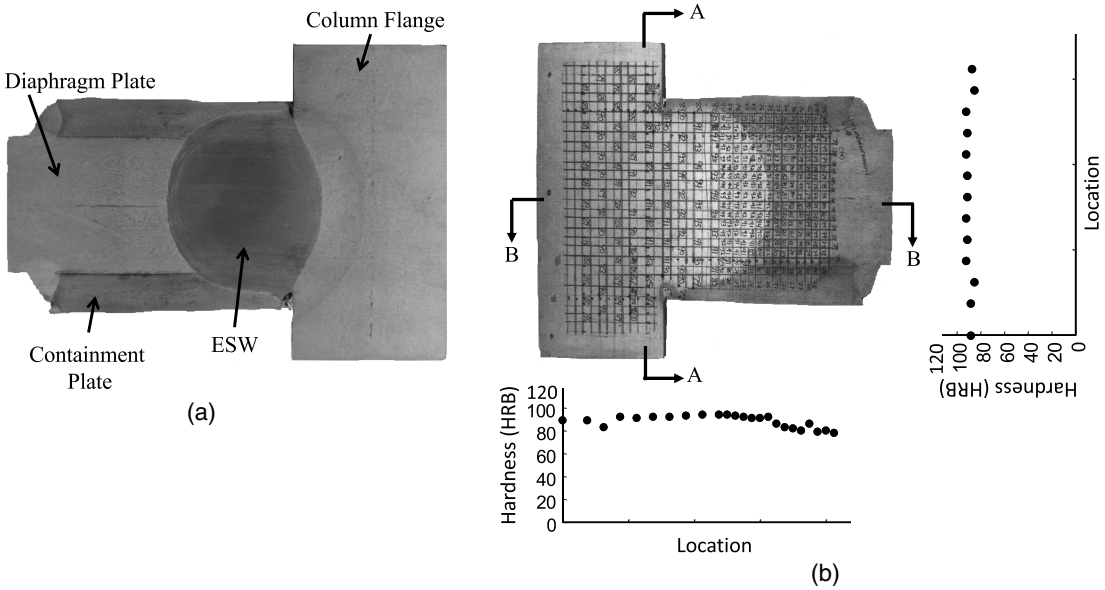

Fig. 9. Specimen 1 ESW joint: (a) macroetched surface; and (b) Rockwell B scale hardness.

(3) reducing the wire feed speed from 88–110 to 83–86 in./min. These modifications permitted a slower fill rate while maintaining similar voltage, with the intent to disperse the weld zone more evenly and eliminate the notches previously discussed.

Reduced Beam Section

AISC 358 specifies the cut dimension c for an RBS as a function of the beam flange width, which ranges from a minimum of 10% to a maximum of 25%. To reduce the force demand to the ESW joints, it was decided to increase the c dimension (Table 2) such that the total reduction of beam flange width was increased from 31% for Specimens 1 and 2 to 49% for Specimen 3. Additionally, the b dimension was increased from 616 mm (24.25 in.) to 762 mm (30.0 in.) for Specimen 3 while maintaining the same radius of cut. The a dimension remained unchanged.

Beam Web Weld Access Hole Geometry

The standard weld access hole profiles specified in AWS D1.1 were used for Specimens 1 and 2. Although Chen et al. (2004) showed that the force demand at the weld access hole was about the same

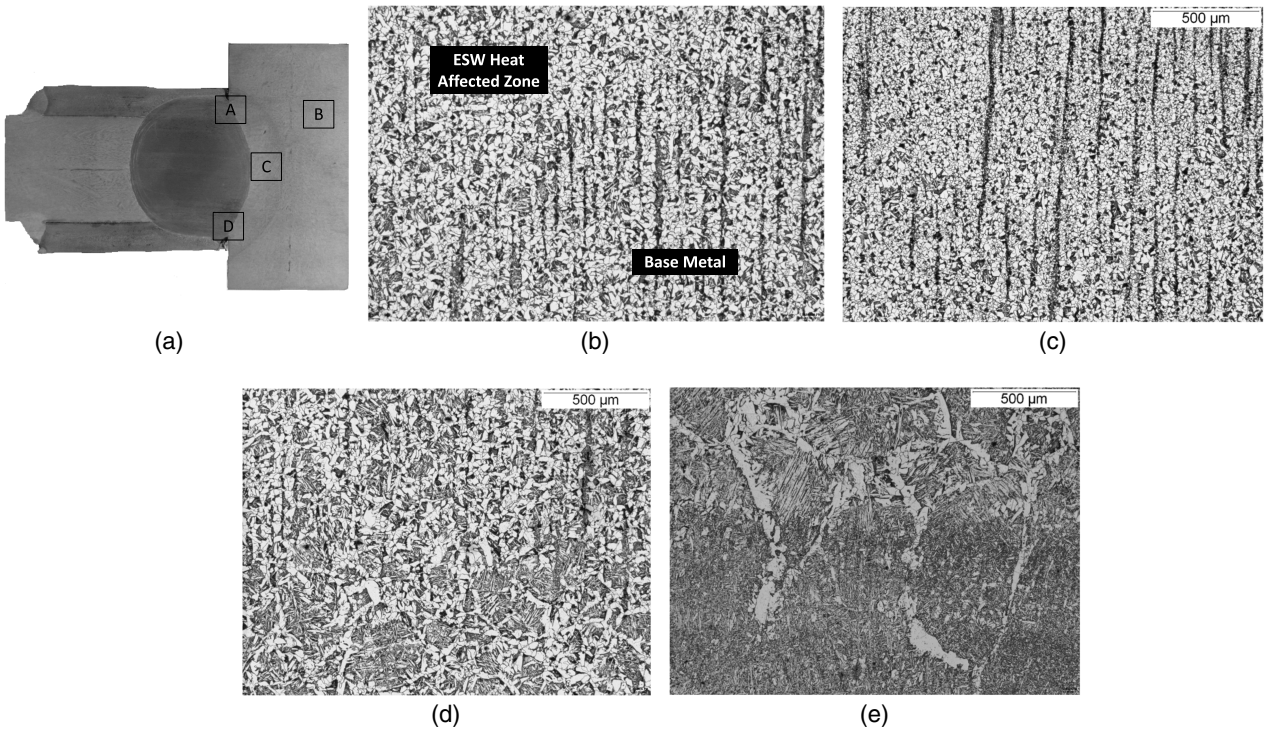

Fig. 10. Microstructure of Specimen 1 ESW joint: (a) designation for metallurgical mounts; (b) Detail A (HAZ-column base metal interface); (c) Detail B (column base metal); (d) Detail C (HAZ); and (e) Detail D (HAZ-weld metal interface).

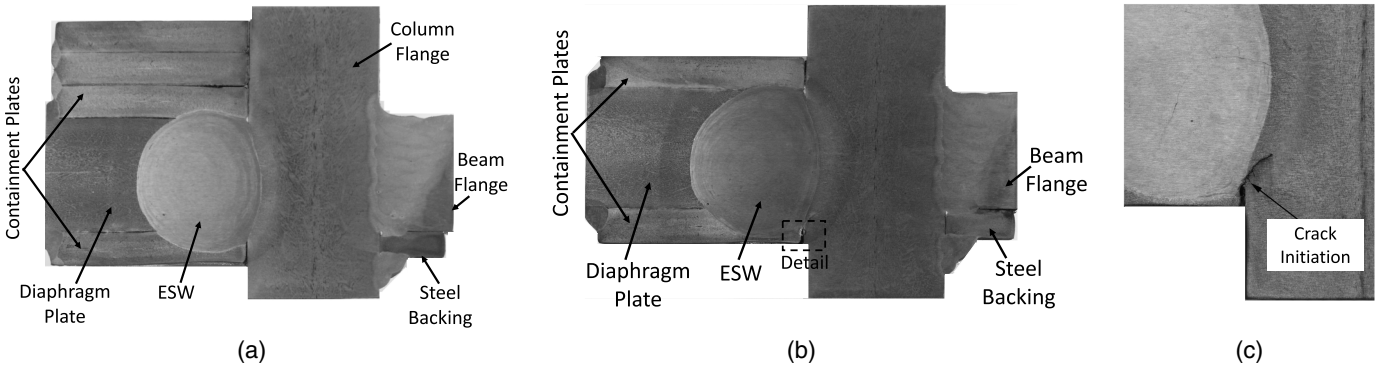

Fig. 11. Specimen 2 ESW joint at beam top flange level: (a) east end; (b) middle; and (c) detail showing the notch condition.

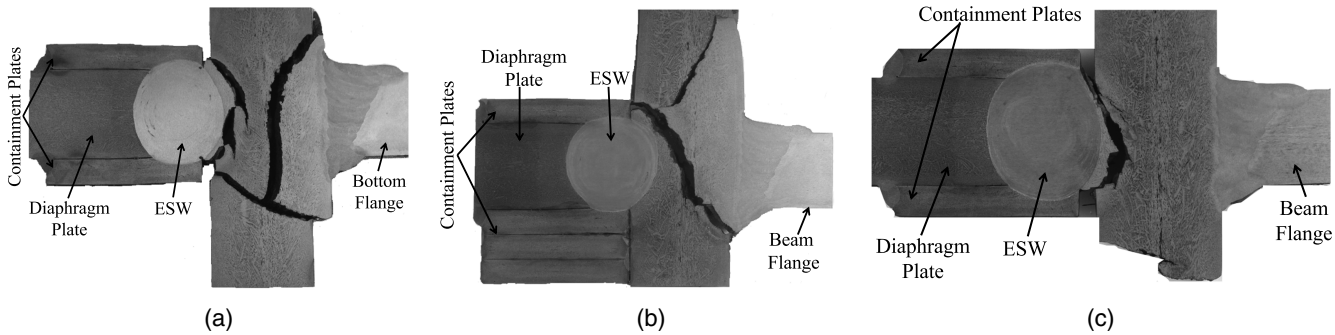

Fig. 12. Specimen 2 ESW joint at beam bottom flange level: (a) east end; (b) west end; and (c) middle.

for both the wide-flange and box columns, to be prudent it was decided to use the improved profile for Specimen 3 (Fig. 13) per Fig. 6.2 in AWS D1.8. The use of a longer weld access hole geometry also permitted easier access for the weld root back gouging of the top flange and the placement of reinforcing fillet weld.

Top Flange Steel Backing Removal

For SMF connections, AISC 358 requires removal of steel backing, backgouging the root pass, and providing a reinforcing fillet weld for the bottom flange CJP weld. At the top flange, steel backing is permitted to be left in place but with a reinforcing fillet weld placed directly beneath the steel backing to the face of the column flange. This relaxed requirement for top flange CJP weld treatment, which was mainly based on testing of moment connections with W-shaped columns in strong-axis bending, was followed in the simulated field welding of Specimens 1 and 2.

When box columns are used, however, a higher percentage of the beam moment is transmitted to the column through the flanges because the web is less effective in transmitting moment (Kim and Oh 2007). Furthermore, the stress concentration at the beam flange welds is the highest near the tips of the flange width (Chen et al. 2004). This combined effect likely resulted in the cracking of the welds at these locations in Specimens 1 and 2 [Figs. 5(b) and 6(c)]. As noted previously, testing showed that initial cracking at the top flange tips started at the 0.015-rad drift angle cycles and gradually increased with increasing drift. Although these cracks did not lead to complete fracture of the connections in the first two specimens, it was judged that the AISC 358 requirement to permit steel backing to be left in place was not conservative when large box columns were used. To improve connection performance and decrease the risk of an unfavorable brittle failure mode, the top flange backing bar was subjected to the same requirements as the bottom flange.

Test Results of Specimen 3

Specimen 3 successfully underwent two cycles at 0.05 rad story drift angle and exhibited a ductile RBS behavior with expected yielding and local web and flange buckling in the RBS region [Fig. 14(a)]. With the improved measures mentioned previously, brittle fracture of the connection did not occur. Removal of the steel backing at the top flange also was found to be effective at mitigating the crack development at the beam tips that occurred in Specimens 1 and 2. The beam eventually experienced ductile fracture in the beam top flange due to low-cycle fatigue during the first cycle at 0.06 rad story drift angle [Fig. 14(b)]. The global response in Fig. 4(c) demonstrates the overall ductility of the connection; the connection met the AISC 341 acceptance criteria.

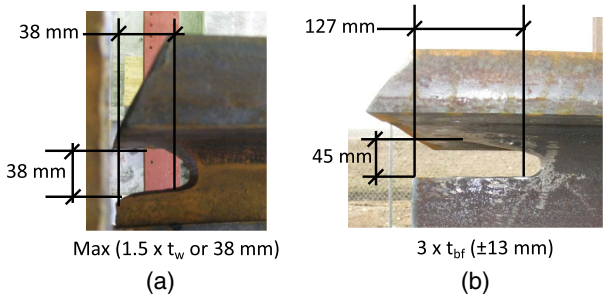

Fig. 13. Beam web weld access hole geometry: (a) Specimens 1 and 2; and (b) Specimen 3.

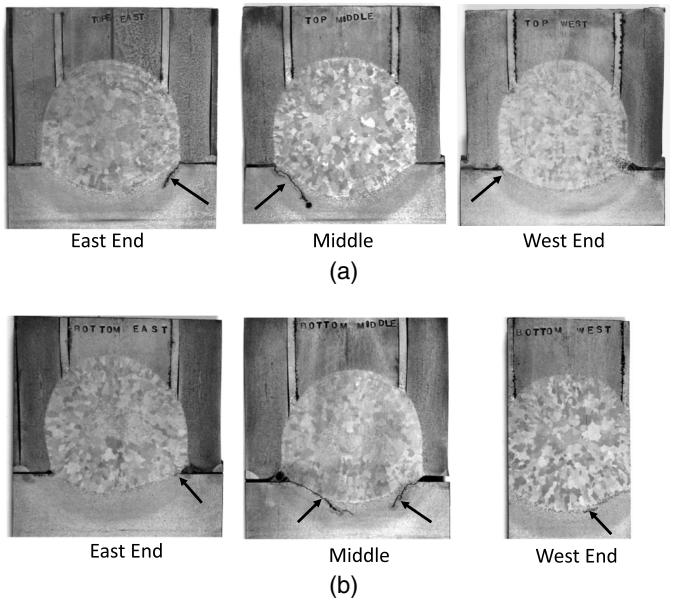

Fig. 15. Specimen 3 ESW joints: (a) top flange level; and (b) bottom flange level.

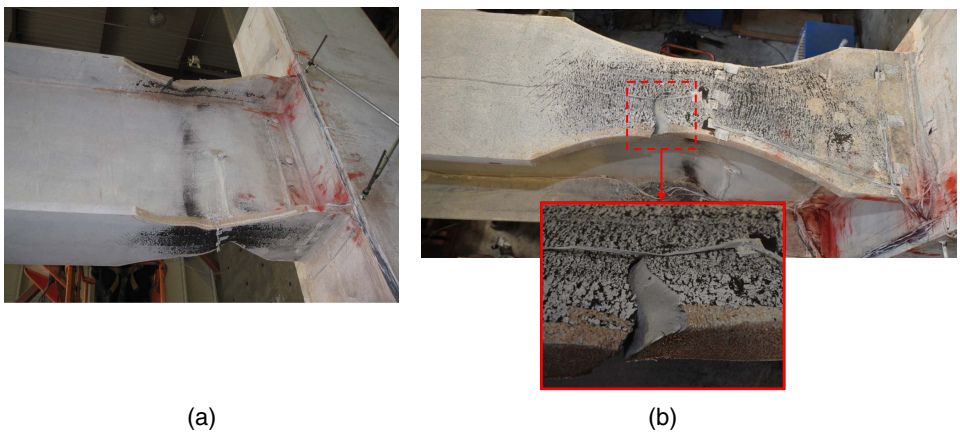

Fig. 14. Specimen 3: (a) yielding and buckling pattern at 0.05 rad drift; and (b) beam top flange fracture at 0.06 rad drift.

Brittle fracture, such as that observed in the first two specimens, was not observed. The ESW joints of Specimen 3 also were examined for comparison after cyclic testing. Although modification of the containment plates in the ESW design allowed for a somewhat wider weld–column plate interface, which helped to delay crack initiation, it still was not sufficient to eliminate the notch-like condition. Fig. 15 shows that cracks still developed.

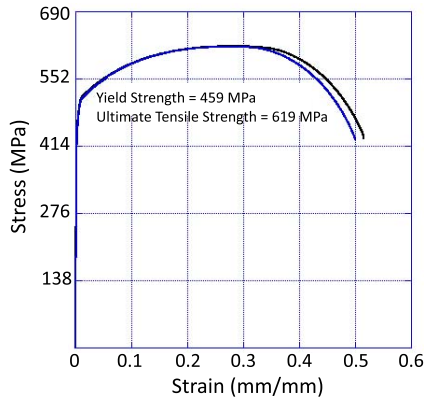

Fig. 16. Specimen 3 ESW metal stress versus strain curves.

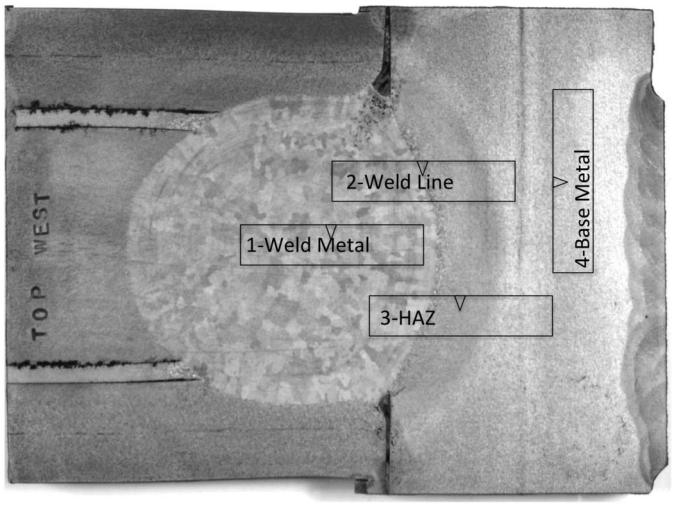

Fig. 17. Specimen 3 Charpy V-notch impact sample location map.

In addition to weld macrostructure, detailed mechanical property analyses of the weld metal, weld-line fusion region, heat affected zone, and column base metal were undertaken from the extracted samples. First, two tensile specimens [consistent with ASTM E8 (ASTM 2016)] were sectioned from the ESW region at the beam top flange level, with the longitudinal axis of the tensile specimen aligned parallel to the length of the weld. The stress-strain data from these two tests are shown in Fig. 16. The average yield stress and tensile strength were 459 MPa (66.5 ksi) and 619 MPa (89.7 ksi), respectively; the total elongation was nearly 50%. These properties were similar to or even slightly better than those of the column flange plate.

Charpy impact specimens were sectioned from four parallel slices through the ESW at the beam bottom flange level. The sections for the Charpy specimens were taken from parallel slices [approximately 13 mm (½ in.) thick] between the east and middle sections. From each of these four slices, four different Charpy samples were extracted. Fig. 17 shows the approximate locations where the samples were extracted, with the notch location being the critical location. Charpy sample #1 was taken from within the weld metal, ensuring that the notch was located entirely within the weld metal region. Charpy sample #2 was sectioned such that the notch was located as close to the weld-line region as possible. Charpy sample #3 was sectioned to ensure that the notch was located within the HAZ of the weld, and Charpy sample #4 was removed from the column flange plate but aligned such that the notch was perpendicular to the rolling direction of the flange plate. The results of the Charpy testing are summarized in Table 4. These results indicated that the weld-line region had a microstructure with the lowest fracture toughness. Therefore, cracks which nucleated at the stress concentration associated with the containment plates propagated along the weld-line region because it had the lowest fracture resistance.

The nondeformed portions of the tested Charpy samples were used to perform a mechanical testing known as stress-strain microprobe (SSM) testing (Haggag et al. 1997), which involves repeated and successively deeper indentations made into the sample surface. The computed yield stress and tensile strength values in Table 5 indicated that the weld-line region had the lowest yield stress.

Table 4. Specimen 3 Charpy V-notch impact values at 21°C (70°F) [J (ft-lb)]

Sample	Location 1 (weld metal)	Location 2 (weld line)	Location 3 (HAZ)	Location 4 (column base metal)
Sample A	95.6 (70.5)	40.0 (29.5)	180.3 (133.0)	181.7 (134.0)
Sample B	89.5 (66.0)	28.5 (21.0)	179.0 (132.0)	164.0 (121.0)
Sample C	92.2 (68.0)	27.1 (20.0)	217.0 (160.0)	162.7 (120.0)
Sample D	130.2 (96.0)	74.6 (55.0)	150.5 (111.0)	162.7 (120.0)
Average	101.8 (75.1)	42.6 (31.4)	181.7 (134.0)	167.9 (123.8)
Standard deviation	19.0 (14.0)	22.1 (16.3)	27.3 (20.1)	9.2 (6.8)

Table 5. Specimen 3 stress-strain microprobe test results

	Weld metal		Weld line		HAZ		Column base metal	
Strength	1a	1b	2a	2b	3a	3b	4a	4b
Yield stress [MPa (ksi)]	466 (67.6)	461 (66.8)	417 (60.5)	410 (59.5)	500 (72.5)	477 (69.2)	531 (77.0)	513 (74.4)
Tensile strength [MPa (ksi)]	618 (89.6)	623 (90.3)	727 (105.5)	769 (111.5)	829 (120.2)	763 (110.7)	803 (116.4)	770 (111.7)

Summary and Conclusions

Three full-scale RBS moment connections with a built-up box column for special moment frame application were cyclically tested with the loading sequence specified in AISC 341. The beam size (W36 × 302) nominally met the prequalification limit of AISC 358; however, the column size [610 × 914 mm (24 × 36 in.)] with 51-mm-thick (2 in.) plates exceeded the box column width or depth prequalification limit of 610 mm (24 in.). Diaphragm plates (i.e., continuity plates) were installed inside the column at the beam top and bottom flange levels. These plates were connected to the column with complete-joint-penetration groove welds; three sides were made with the flux-cored arc welding process and the last (i.e., closing) side was made with the electroslag narrow-gap welding process. The beam framed into the column on the ESW side. A992 steel was specified for the beams and A572 Gr. 50 steel was specified for all plates. The first two specimens, which were nominally identical, experienced brittle fracture. Based on the failure mode, modifications were made to Specimen 3. After the test, the box column of each specimen was sectioned to extract the welded joints of the diaphragm plates for further examination. The following conclusions can be made from this test program:

1. Cyclic testing clearly showed that the performance of the ESW joints inside the box column was crucial for the integrity of the moment connection. Brittle fracture of the first two nominally identical specimens started from inside the built-up box column and was caused by a notch condition of the ESW joints. The notch existed between the innermost containment plates and the column flange plate (Figs. 11 and 12). Brittle fracture of Specimen 1 occurred soon after two cycles at a story drift angle of 0.04 rad were completed. Specimen 2 did not complete one cycle at 0.04 rad drift.
2. Specimen 3 was able to sustain one cycle at 0.06 rad drift angle and exhibited a ductile response. Two primary factors contributed to the improved performance: (1) modifications made to ESW joint weld detail and weld process, especially the use of beveled containment plates and additional spacer (i.e., shim) plates [Fig. 3(b)], delayed the initiation of cracks; and (2) an increased reduction of the beam flange width in the RBS region (Table 2) reduced the flexural moment demand at the column face by approximately 17%. Other factors included the use of a longer beam web weld access hole geometry per AWS D1.8 and the removal of beam top flange CJP steel backing.
3. Rockwell B scale hardness tests showed that the hardness of FCAW and ESW joints used to connect the diaphragm plate to box column plates was similar. Results of Charpy V-notch tests revealed that the weld-line fusion zone had the lowest fracture toughness compared with the ESW weld and heat-affected zone.
4. Although using the beveled containment plates and spacer plates for making ESW joints was found to be effective in delaying the fracture mentioned in Conclusion 1, cracking still occurred due to the persistence of a notch-like condition. Further research is needed to improve this weld detail.
5. AISC 358 permits steel backing of the top flange weld to remain if a reinforcing fillet weld is added beneath the steel backing. When a box column is used, it is well-known that the stress concentration is highest at the flange tips; testing of the first two specimens demonstrated this with the initiation of cracks at the flange tips. Based on the testing of Specimen 3, it is recommended that the same steel backing requirement as in the bottom flange be adopted when a box column is used. It is also recommended, as was done in Specimen 3, that the AWS D1.8 weld access hole be used.

Acknowledgments

The test program was sponsored by Judicial Council of California (JCC). The authors are grateful to Dr. Ker-Chun Lin at the National Center for Research on Earthquake Engineering in Taiwan for sharing a patented detail for ESW welding that is commonly used for ESW welding in Taiwan, and to Arcmatic Welding for sharing their development of narrow-gap electroslag welding. Professor Kenneth Vecchio, Department of Nanoengineering, University of California San Diego, assisted in characterizing the mechanical properties of the welded joints.

References

AISC. 2010a. *Prequalified connections for special and intermediate steel moment frames for seismic applications*. AISC 358. Chicago: AISC.

AISC. 2010b. *Seismic provisions for structural steel buildings*. ANSI/AISC 341. Chicago: AISC.

AISC. 2010c. *Specification for structural steel buildings*. ANSI/AISC 360. Chicago: AISC.

AISC. 2011. *Prequalified connections for special and intermediate steel moment frames for seismic applications: Supplement No. 1*. ANSI/AISC 358s1. Chicago: AISC.

Anderson, J. C., and R. R. Linderman. 1991. *Steel beam to box column connections*. Rep. No. CE 91-03. Los Angeles: Dept. of Civil Engineering, Univ. of Southern California.

ASTM. 2016. *Standard test methods for tension testing of metallic materials*. ASTM E8/E8M-16a. West Conshohocken, PA: ASTM.

AWS (American Welding Society). 2008. *Bridge welding*. AASHTO/AWS D1.5M/D1.5. Miami: AWS.

AWS (American Welding Society). 2009. *Structural welding code–seismic supplement*. AWS D1.8/D1.8M. Miami: AWS.

AWS (American Welding Society). 2011. *Structural welding code–steel*. AWS D1.1/D1.1M. Miami: AWS.

Chambers, J. J., W. L. Bong, and B. R. Manning. 2014. "Electroslag welding solutions for high-seismic regions." In *Proc., SEAOC Annual Convention*. Sacramento, CA: Structural Engineers Association of California.

Chen, C. C., C. C. Lin, and C. L. Tsai. 2004. "Evaluation of reinforced connections between steel beams and box columns." *Eng. Struct.* 26 (13): 1889–1904. https://doi.org/10.1016/j.engstruct.2004.06.017.

Chen, C.-C., and Y-C. Liang. 2011. "The effects of electroslag welding on material properties of box column plates." *Int. J. Steel Struct.* 11 (2): 171–189. https://doi.org/10.1007/s13296-011-2006-2.

Engelhardt, M. D., T. Winneberger, A. J. Zekany, and T. Potyraj. 1998. "Experimental investigation of dogbone moment connections." *Eng. J.* 35 (4): 128–139.

FEMA. 2000a. *Recommended seismic design criteria for new steel moment-frame buildings*. FEMA-350. Washington, DC: FEMA.

FEMA. 2000b. *State-of-the-art report on connection performance*. FEMA-355D. Washington, DC: FEMA.

Haggag, F. M., J. A. Wang, M. A. Sokolov, and K. L. Murty. 1997. "Use of portable/in situ stress-strain microprobe system to measure stress-strain behavior and damage in metallic materials and structures." In *Nontraditional Methods of Sensing Stress, Strain, and Damage in Materials and Structures*, edited by G. F. Lucas and D. A. Stubbs. West Conshohocken, PA: ASTM.

Kim, T., B. Stojadinovic, and A. S. Whittaker. 2008. "Seismic performance of pre-Northridge welded steel moment connections to built-up box columns." *J. Struct. Eng.* 134 (2): 289–299. https://doi.org/10.1061/(ASCE)0733-9445(2008)134:2(289).

Kim, Y.-J., and S.-H. Oh. 2007. "Effect of the moment transfer efficiency of a beam web on deformation capacity at box column-to-H beam connections." *J. Constr. Steel Res.* 63 (1): 24–36. https://doi.org/10.1016/j.jcsr.2006.02.009.

Lee, P., R. Garai, A. Tsui, and Y. Hua. 2016. "Special moment frame qualifications: RBS to box column." In *Proc., 85th Annual Convention*. Sacramento, CA: SEAOC.

Nakashima, M., C. W. Roeder, and Y. Maruoka. 2000. "Steel moment frames for earthquakes in United States and Japan." *J. Struct. Eng.* 126 (8): 861–868. https://doi.org/10.1061/(ASCE)0733-9445(2000)126:8(861).

Ozkula, G., and C. M. Uang. 2014. *Cyclic testing of steel RBS moment connections with built-up box column for the San Diego Central Courthouse*. Rep. No. TR-13/01. La Jolla, CA: Dept. of Structure Engineering, Univ. of California San Diego.

Ricles, J. M., J. W. Fisher, L.-W. Lu, and E. J. Kaufmann. 2002a. "Development of improved welded moment connections for earthquake-resistant design." *J. Constr. Steel Res.* 58 (5–8): 565–604. https://doi.org/10.1016/S0143-974X(01)00095-5.

Ricles, J. M., C. Mao, L. W. Lu, and J. W. Fisher. 2002b. "Inelastic cyclic testing of welded unreinforced moment connections." *J. Struct. Eng.* 128 (4): 429–440. https://doi.org/10.1061/(ASCE)0733-9445(2002)128:4(429).

Song, Y. H., T. Ishii, Y. Harada, and K. Morita. 2011. "Study on fracture behavior of electro-slag welded joints in beam-to-built-up box column connections." In *Proc., 6th Int. Symp. on Steel Structures*. Seoul: Korean Society of Steel Construction.

Tsai, K.-C., K.-C. Lin, S.-J. Juang, C.-H. Li, and C.-H. Lin. 2015. "Research and practice on seismic design of welded steel beam-to-box column moment connections in Taiwan." In *Proc., Symp. on Future Development of Seismic Design*. Hong Kong: Hong Kong Institute of Steel Construction.

Tsai, K.-C., K.-C. Lin, and M.-C. Liu. 1992. "Seismic behavior of steel beam-to-box column connections." In *Proc., 10th World Conf. on Earthquake Engineering*. Rotterdam, Netherlands: A.A. Balkema.

Yu, Q. S., and C.-M Uang. 2001. "Effects of lateral bracing and system restraint on the behavior of reduced beam section moment frame connections." *Steel Compos. Struct.* 1 (1): 145–158. https://doi.org/10.12989/scs.2001.1.1.145.